

On the Presence of Liquid in Earth's Inner Core

S. C. Singh,^{1,2*} M. A. J. Taylor,² J. P. Montagner¹

Seismological studies indicate that the inner core of Earth is anisotropic for compressional waves (*P* waves), and has low shear wave (*S* wave) velocity, and high seismic attenuation. Using an effective medium theory for composite materials, we show that the presence of a volume fraction of 3 to 10% liquid in the form of oblate spheroidal inclusions aligned in the equatorial plane between iron crystals is sufficient to explain the aforementioned seismic phenomena. Variation of *S*-wave velocity between the polar axis and equatorial plane is more sensitive to the addition of liquid than that of *P* waves. The liquid could arise from the presence of dendrites or a mixture of elements other than iron that exist in liquid form under inner-core conditions.

On the basis of the lack of any observed *S* waves from the deeper part of Earth, in 1929 Sir Harold Jeffreys (1) proposed that the core of Earth consisted of fluid. In 1935, Lehmann (2) introduced the concept of the inner core and suggested that it could be solid. Since then, the solidity of the inner core has been reaffirmed by the observations of reflected phases from the inner core boundary (ICB) (3), normal modes (4), and more recently by the presence of transmitted *S*-wave phases (5, 6). However, these results do not rule out the possibility of the presence of a small amount of fluid in the inner core. Although this notion has been qualitatively put forward before for individual seismic observations (7–9), we quantitatively demonstrate here that the seismic data can be explained by the presence of a small amount of fluid in the inner core.

We limit our consideration to a few basic seismic parameters that can be compared with observations from the inner core, namely, *P*- and *S*-wave velocities and attenuation in the vicinity of the ICB, and average *P*-wave anisotropy. Accordingly, we employ relatively simple models that are isotropic or transversely isotropic. The *P*-wave velocity in the core is well constrained, jumping from 10.29 km s⁻¹ to 11.04 km s⁻¹ at the ICB, and then increasing linearly to 11.26 km s⁻¹ at the center of Earth (10). The *S*-wave velocity is not so well constrained but is <3.65 km s⁻¹ at the ICB (4–6). Seismic attenuation studies suggest that at least the outer part of the inner core has high attenuation with a quality factor (11) of 200 to 400 for *P* waves (7, 12) and 100 to 200 for *S* waves (7, 12, 13). Several studies of *P* waves suggest that the inner core of Earth is elastically anisotropic (14–18), with the *P*-wave velocity along the

pole axis being 3 to 4% higher than that in the equatorial plane, although there are studies indicating the absence of anisotropy (19). It has also been suggested that the *P*-wave anisotropy is in the opposite sense to the *P*-wave attenuation anisotropy (20, 21).

To shed light upon the composition, and hence the evolution, of the inner core, it is necessary to relate these seismic properties to plausible materials at inner-core temperatures (4000 to 8000 K) and pressures (330 to 360 GPa). The hexagonal close-packed (hcp) form of solid Fe is considered to be the dominant material in the inner core (22–26). The density and elastic parameters of hcp Fe have been calculated both experimentally (25–28) and theoretically (29) at high pressure and room temperature. These results can explain the *P*-wave anisotropy in the inner core, but they overestimate the *P*- (25, 26) and *S*-wave (29) velocities. The anisotropy in the inner core could also originate from a low-order convection (30, 31) or solidification texturing (32). If the inner core consists of pure solid Fe crystals (29), then seismic attenuation would be small, with a quality factor of the order of tens of thousands. We postulate that fluid inclusions might be responsible for these discrepancies. Using an effective medium theory for a composite material, we quantify the amount, geometry, and form of the fluid inclusions that would be required to simultaneously explain the presence of seismic anisotropy, high attenuation, and low *S*-wave velocity, and then suggest that the inner core might be partially molten.

We used a differential effective medium theory (33–36), where liquid inclusions are introduced incrementally into a solid background matrix to produce a two-phase composite. The inclusions are introduced in the form of spheroids with semi-axes *a* and *c* (for Cartesian coordinates *x*, *y*, and *z*, $x^2/a^2 + y^2/a^2 + z^2/c^2 = 1$; $x, y \leq a, z \leq c$), and which have a circular cross section in the *xy* plane. The existence of an analytic solution for the changes in elastic properties that are intro-

duced (37) and the fact that the shape of the spheroid can be defined by a single parameter, the ratio of its semi-axes *a/c*, make this choice of geometry advantageous. We consider spheroids with aspect ratios varying from 1 (spheres) to 100 ($a > c$, flat disks) to 0.01 ($a < c$, thin fibers). The solid background material can be isotropic or anisotropic, and the liquid inclusions can either be oriented randomly in the medium (isotropic) or be aligned along one direction (anisotropic).

To model the solid background material, we used the theoretically calculated elastic parameters of the hcp Fe crystal at 330 GPa (29). These values are for room temperature, and although they might vary with increasing temperature (25), the trends we present remain valid at higher temperatures. When considering the effect of the liquid inclusions, we took the properties of the outer core at the ICB (10, 25), which is thought to consist of liquid Fe. Any other liquid with similar seismic properties could be considered. We assumed that the inclusions are not connected to one other, which is valid for the low concentrations considered here. If the inclusions are aligned along a particular direction, in order to maintain the transversely isotropic properties exhibited by the hcp Fe, the inclusions must be aligned with their *c* axes parallel to the symmetry axis of the background medium. The symmetry axis of the hcp Fe and the *c* axes of the inclusions are therefore assumed to be aligned with the polar axis of Earth.

Adding spherical (*a/c* = 1) inclusions to an isotropic background-matrix material does not introduce any *P*-wave anisotropy, and so the composite material remains isotropic for all melt fractions (Fig. 1A). However, the *P*-wave velocity decreases smoothly with the increase of melt fraction [Web fig. 1 (38)]. Adding inclusions with *a/c* ≠ 1 produces a transversely isotropic composite material, with the anisotropy increasing or decreasing with the increase of melt fraction for *a/c* < 1 and *a/c* > 1, respectively (Fig. 1A). In order to produce a *P*-wave anisotropy of 3% as suggested by the seismic data, one would require >14% of liquid in a fiber form (*a/c* < 1) aligned along the polar axis.

Addition of isotropic spheres of melt to an anisotropic background-matrix of hcp Fe (29), where the *P*-wave velocity along the polar (symmetry) axis is faster than that in the transverse direction, does not alter the anisotropy very much with increasing melt fraction (Fig. 1B). Addition of aligned liquid inclusions with *a/c* ≠ 1 has the same effect as in the isotropic case, but now the initial anisotropy is non-zero, leading to positive values for *P*-wave anisotropy up to about 11.75% melt (Fig. 1B). If we assume that the inner-core anisotropy is somewhere between 0 and 3%, then we would require 0 to 14% of aligned liquid inclusions with *a/c* < 1 (fibers) for an

¹Département de Sismologie, Institut de Physique du Globe de Paris, 4 Place Jussieu–75252, Paris Cédex 05, France. ²Bullard Laboratories, University of Cambridge, Cambridge, CB3 0EZ, UK.

*To whom correspondence should be addressed. E-mail: singh@ipgp.jussieu.fr

isotropic matrix or 0.5 to 11.75% of aligned inclusions with $a/c > 1$ (disks) for an anisotropic matrix. If the inclusions were randomly oriented, they would have little or no effect on the P -wave anisotropy. These results are therefore consistent both with cases of the proposed presence (14–18) and absence (19) of anisotropy.

From the existing seismic data, we only have estimates for the vertically polarized S -wave (SV) velocity and have no constraints on the horizontally polarized S -wave (SH) velocity. The effect on the SV velocity of adding liquid inclusions to an anisotropic background matrix, aligned with their c axes along the polar direction and $a/c = 0.1$ or 0.01 , differs little from adding spherical liquid inclusions, because these shapes are relatively rigid in response to shear in the vertical plane (Fig. 2A). However, aligned liquid inclusions with $a/c = 10$ or 100 have a devastating effect on the S -wave velocity, because the inclusions are weak when subjected to shear in the vertical plane, thus strongly decreasing the SV velocity with the addition of only a few percent of melt (Fig. 2A). For instance, only $\sim 3\%$ melt fraction of inclusions of $a/c = 100$ is sufficient to reduce the S -wave velocity from 6 km s^{-1} of the pure solid hcp Fe to the seismically observed value

of 3.65 km s^{-1} . For inclusions of $a/c = 10$, $\sim 17.5\%$ melt is required. The reduction in SH velocity in the equatorial plane that arises from adding liquid inclusions of any aspect ratio is much less (Fig. 2B) because the inclusions are relatively rigid in their plane of symmetry. These results are similar for an isotropic starting material (Web fig. 2). Therefore, to reduce the SV velocity significantly, the inclusions must have aspect ratios > 1 , equivalent to aligned disks lying in the equatorial plane.

The variation of velocity with propagation angle between the polar axis (0°) and the equatorial plane (90°) for a melt fraction of 5% and $a/c = 10$ (Fig. 3) highlights the effect of a relatively low liquid fraction within the range of our final estimate of values that are consistent with the seismic observations. We compared our results with those of Stixrude and Cohen (29) for pure hcp Fe. The P -wave velocity and anisotropy variation with angle differs very little from that of pure Fe with the addition of 5% liquid, and the greatest difference in normalized P -wave velocity is only $\sim 1.5\%$. The effect on the S -wave velocity of adding only a small amount of liquid is striking. The SV velocity of the composite is $\sim 8\%$ greater than that for pure Fe at 45° , and the SH velocity of the composite is $\sim 12\%$ greater than that for pure Fe at 90° . These results suggest that a more complete knowledge of the S -wave velocity and S -wave anisotropy are key factors in constraining the model of the inner core.

In the absence of any knowledge of the S -wave anisotropy, we turn our attention to

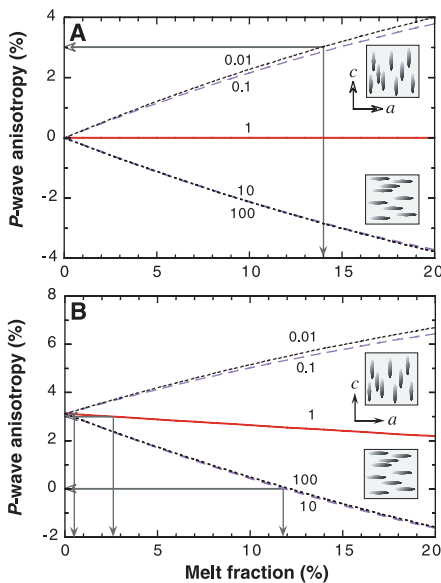


Fig. 1. Variation of P -wave anisotropy $[(C_{3333} - C_{1111})/\rho V_p^2]$ against melt fraction for liquid inclusions with $a/c = 1$ (spheres), 10 and 100 (flat disks), and 0.1 and 0.01 (elongated fibers). Sense of alignment and shape are indicated by schematic on right. C_{ijkl} are components of the stiffness tensor where **3** is coincident with the polar axis and **1** and **2** lie in the equatorial plane, ρ is the density of the composite, and V_p is the P -wave velocity of the 100% solid matrix in the **3** direction. Starting materials are (A) an isotropic solid and (B) an anisotropic solid with hcp symmetry (29). Arrows indicate range of melt fraction consistent with 0 to 3% anisotropy.

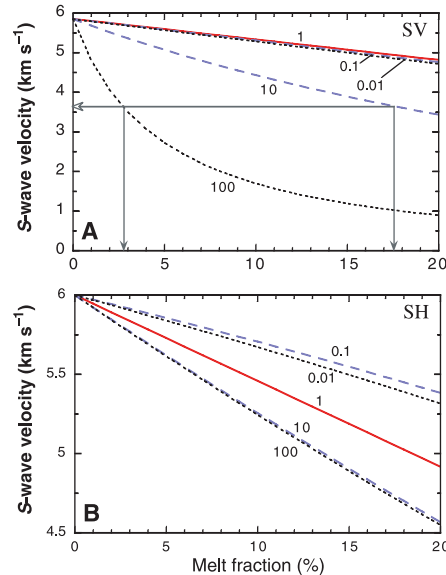


Fig. 2. Variation of S -wave velocity against melt fraction for liquid inclusions of the same range of aspect ratios as in Fig. 1. Starting matrix material is anisotropic hcp Fe (29). (A) SV velocity ($V_{SV} = \sqrt{C_{2323}/\rho}$). Arrows indicate melt fractions consistent with $V_S = 3.65 \text{ km s}^{-1}$. (B) SH velocity in equatorial plane ($V_{SH} = \sqrt{C_{1212}/\rho}$).

seismic attenuation. We apply an extension of a theory developed by Hudson *et al.* (39) to calculate the P - and S -wave attenuation, Q_P^{-1} and Q_S^{-1} , respectively (40). To minimize the number of parameters considered, we present results for the isotropic case where the background material and liquid are isotropic and the liquid inclusions are added with random orientations. Although there is uncertainty in all the parameters in the expressions for the attenuation (40), by far the least well constrained is the viscosity of the liquid η_l , which, based on estimates for the viscosity of the liquid in the outer core, could be anywhere between 10^{-1} and $10^8 \text{ kg m}^{-1} \text{ s}^{-1}$ (41). Thus, we treat this as a variable in our computations and present results of attenuation for the whole range of viscosities of interest. We assumed that the dominant frequency range of the seismic waves was 0.2 to 1.5 Hz and the average length of the inclusions was 10^{-3} to 10^{-6} times the seismic wavelength. The attenuation shows a maximum peak at a viscosity of about $250 \text{ kg m}^{-1} \text{ s}^{-1}$ (Fig. 4) and diminishes completely for lower and higher viscosities. This is intuitive, because one would not expect any attenuation if the liquid in the inclusions is like water ($\eta_l = 10^{-2} \text{ kg m}^{-1} \text{ s}^{-1}$) since it would diffuse and reequilibrate the pressure differential almost instantaneously compared to the time for the wave to pass through the medium. Similarly, if the viscosity is high (for example, $\eta_l = 10^8 \text{ kg m}^{-1} \text{ s}^{-1}$), the composite responds as a purely elastic material on the time scale of the seismic wave and there is no attenuation. For a fixed viscosity, the P - and S -wave attenuation increase linearly with increasing liquid content up to 10% melt fraction.

At fixed viscosity, for a given melt fraction the attenuation decreases with increasing aspect ratio and is most pronounced for spherical inclusions (Fig. 5, A and B). The attenuation is a maximum for $\eta_l = 100 \text{ kg m}^{-1} \text{ s}^{-1}$.

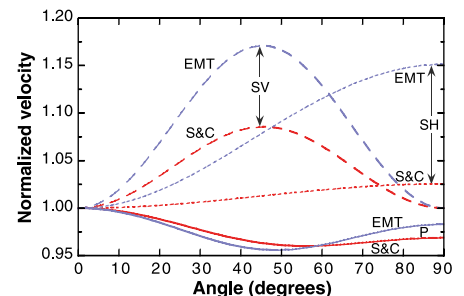


Fig. 3. Variation of P -wave (solid lines), SV (long dashed lines), and SH (short dashed lines) velocity with the direction of propagation from the polar axis (0°) to the equatorial plane (90°). Compared are results from figure 1(B) of Stixrude and Cohen (29) (red lines, "S&C") and effective medium theory for 5% melt fraction and $a/c = 10$ (blue lines, "EMT"). Velocities are normalized by value along polar direction (for S&C: $V_p = 12.13 \text{ km s}^{-1}$, $V_S = 5.84 \text{ km s}^{-1}$; for EMT: $V_p = 11.83 \text{ km s}^{-1}$, $V_S = 5.07 \text{ km s}^{-1}$).

REPORTS

$m^{-1} s^{-1}$ and decreases for progressively higher and lower viscosities. To explain the seismically observed values of $Q_p^{-1} = 0.05$ and $Q_s^{-1} = 0.01$, one would require ~6 to 8% of liquid inclusions with $\eta_l = 100 \text{ kg m}^{-1} s^{-1}$ and $a/c = 10$, or 12 to 16% of liquid inclusions with $\eta_l = 1000 \text{ kg m}^{-1} s^{-1}$ and $a/c = 10$. Both of these cases are consistent with the P -wave anisotropy and S -wave velocity results. In estimating the attenuation, we assumed that the background material is isotropic. If the background material is composed of aligned hcp Fe crystals, as suggested by Figs. 1 and 2, then the effect of aligned fluid inclusions in the equatorial direction would be the same as that of stratified small-scale scatters (21), which would explain the attenuation anisotropy (20, 21). This is confirmed by the decrease of P -wave anisotropy with the increase of liquid inclusions (Fig. 1). Normal mode studies (13) suggest low attenuation ($Q \sim 3000$) compared to body wave

results (20). Our calculations suggest that this discrepancy could be explained by the frequency-dependence of attenuation from liquid inclusions (Fig. 4) (40).

Although there are several independent parameters controlling the attenuation, P -wave anisotropy, and S -wave velocity, we conclude that a 3 to 10% melt fraction of spheroidal liquid inclusions with an aspect ratio of 10 to 20 (flat disks), aligned with their c axes along the polar axis and with a viscosity of the order of $100 \text{ kg m}^{-1} s^{-1}$, would explain the existing seismic observations. Our model suggests that the S -wave anisotropy in the inner core should be large, of the order of 20%, and the determination of this is important in distinguishing our model from others.

Our estimate of the liquid content in the inner core is based on existing seismic results. As the constraints on values of the S -wave velocity and attenuation are mainly from the outer part of the inner core, we suggest that the

liquid is present at least in the upper few hundred kilometers. It has been proposed that Earth's inner core has formed by gradual solidification of the liquid core as Earth cooled (42), and compositional effects associated with this solidification process can release energy at a rate sufficient to power the geodynamo (43). If the core is not composed of pure Fe, but instead is an uncertain mixture of other elements (30), then it is possible that some elements might be in a liquid state at the inner-core temperature and pressure conditions. It has been suggested (23, 24) that up to 10% sulfur might be present in the inner core. The melting temperature of sulfur is much lower than that of Fe; therefore, it is possible that FeS in liquid form might get trapped in the inner core. Earth's rotation could be the cause of alignment of the liquid in the equatorial plane. The presence of liquid would also increase the inviscidity of the inner core, which might lead to convection (14). A partially molten inner core would have profound implications for the evolution and dynamics of the core.

Fig. 4. P -wave attenuation (Q_p^{-1}) variation with melt fraction and melt viscosity (η_l) [S -wave attenuation (Q_s^{-1}) variation with melt fraction and η_l shown in Web fig. 3]. Both plots reveal a peak at $\eta_l \sim 250 \text{ kg m}^{-1} s^{-1}$. This figure equivalently illustrates the variation in Q_p^{-1} with melt fraction and variable frequency (ω) at fixed η_l (40).

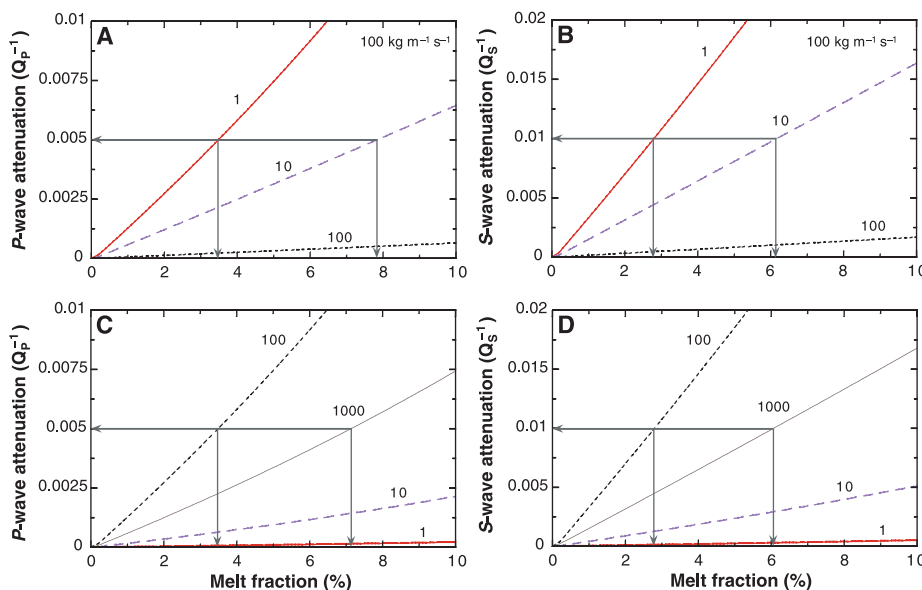
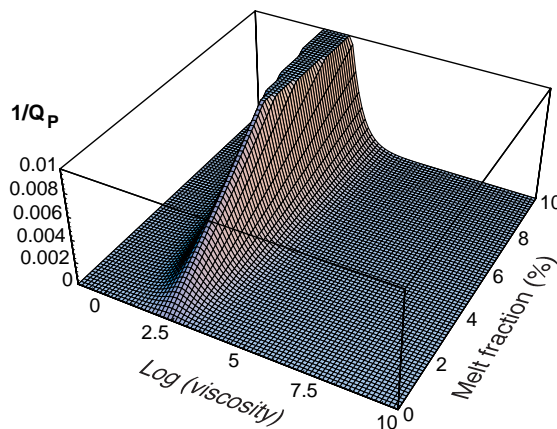


Fig. 5. Variation of (A) Q_p^{-1} and (B) Q_s^{-1} with melt fraction at constant viscosity ($\eta_l = 100 \text{ kg m}^{-1} s^{-1}$) for $a/c = 1, 10, \text{ and } 100$. Variation of (C) Q_p^{-1} and (D) Q_s^{-1} with melt fraction at constant aspect ratio ($a/c = 1$) for viscosities $\eta_l = 1, 10, 100, \text{ and } 1000 \text{ kg m}^{-1} s^{-1}$. Arrows indicate range of melt fraction consistent with observed values for attenuation in the inner core.

References and Notes

1. H. Jeffreys, *The Earth* (Cambridge Univ. Press, New York, 1929), p. 265.
2. I. Lehmann, *Bur. Central Seismol. Int. Ser. A* **14**, 3 (1936).
3. K. E. Bullen, *Ann. Geophys.* **6**, 1 (1953).
4. A. M. Dziewonski and F. Gilbert, *Nature* **234**, 465 (1971).
5. B. R. Julian, D. Davies, R. M. Sheppard, *Nature* **235**, 317 (1972).
6. E. A. Okal and Y. Cansi, *Earth Planet. Sci. Lett.* **164**, 23 (1998).
7. A. Souriau and P. Roudil, *Geophys. J. Int.* **123**, 572 (1995).
8. D. J. Doornbos, *Geophys. J. R. Astron. Soc.* **38**, 397 (1974).
9. D. R. Fearn, D. E. Loper, P. H. Roberts, *Nature* **292**, 232 (1981).
10. B. L. N. Kennett, E. R. Engdahl, R. Buland, *Geophys. J. Int.* **122**, 108 (1995).
11. Quality factor, $Q = 2\pi / (\text{fractional loss of energy per cycle}) = 1/\text{attenuation}$.
12. J. Bhattacharyya, P. Shearer, G. Masters, *Geophys. J. Int.* **114**, 1 (1993).
13. R. Widmer, G. Masters, F. Gilbert, *Geophys. J. Int.* **104**, 541 (1991).
14. A. Morelli, A. M. Dziewonski, J. H. Woodhouse, *Geophys. Res. Lett.* **13**, 1545 (1986).
15. J. H. Woodhouse, D. Giardini, X. D. Li, *Geophys. Res. Lett.* **13**, 1549 (1986).
16. P. M. Shearer, K. M. Toy, J. A. Orcutt, *Nature* **333**, 228 (1988).
17. K. C. Creager, *Nature* **356**, 309 (1992).
18. J. Tromp, *Nature* **366**, 678 (1993).
19. L. Breger, B. Romanowicz, H. Tkalcic, *Earth Planet. Sci. Lett.* **175**, 133 (2000).
20. A. Souriau and B. Romanowicz, *Geophys. Res. Lett.* **23**, 1 (1996).
21. V. F. Cormier, L. Xu, G. L. Choy, *Geophys. Res. Lett.* **25**, 4019 (1998).
22. F. Birch, *J. Geophys. Res.* **57**, 227 (1952).
23. A. Jephcoat and P. Olson, *Nature* **325**, 332 (1987).
24. L. Stixrude, E. Wasserman, R. E. Cohen, *J. Geophys. Res.* **102**, 24729 (1997).
25. J. M. Brown and R. G. McQueen, *J. Geophys. Res.* **91**, 7485 (1986).
26. H. K. Mao, Y. Wu, L. C. Chen, J. F. Shu, A. Jephcoat, *J. Geophys. Res.* **95**, 21737 (1990).
27. H. K. Mao et al., *Nature* **396**, 741 (1998); *Nature* **399**, 280 (1999).
28. S. C. Singh and J.-P. Montagner, *Nature* **400**, 629 (1999).

29. L. Stixrude and R. E. Cohen, *Science* **267**, 1972 (1995).
 30. R. Jeanloz and H. R. Wenk, *Geophys. Res. Lett.* **15**, 72 (1988).
 31. B. Romanowicz, X.-D. Li, J. Durek, *Science* **274**, 963 (1996).
 32. M. I. Bergman, *Nature* **389**, 60 (1997).
 33. O. Nishizawa, *J. Phys. Earth* **30**, 331 (1982).
 34. B. E. Hornby, L. M. Schwartz, J. A. Hudson, *Geophysics* **59**, 1570 (1994).
 35. P. Sheng, *Phys. Rev. B* **41**, 4507 (1990).
 36. M. Jakobsen, J. A. Hudson, T. A. Minshull, S. C. Singh, *J. Geophys. Res.* **105**, 561 (2000).
 37. J. D. Eshelby, *Proc. R. Soc. London Ser. A* **241**, 376 (1957).
 38. Supplemental figures are available at www.sciencemag.org/feature/data/1047337.shl
 39. J. A. Hudson, E. Liu, S. Crampin, *Geophys. J. Int.* **124**, 105 (1996).
 40. From first-order perturbation theory (35), the bulk modulus can be written as $\kappa = \kappa_0 + \phi\kappa_1$, where κ_0 is the bulk modulus of the background matrix, ϕ is the melt fraction of inclusions, and κ_1 is the first term in the expansion that is given by

$$\frac{\kappa_1}{\kappa_0} = -\frac{\kappa_0}{\mu} \frac{4}{3} \left(\frac{\lambda + 2\mu}{\lambda + \mu} \right) \left(\frac{1 + i\omega\tau}{1 + i\gamma\omega\tau} \right) \times \left[1 - \left(\frac{1 - \gamma^{-1}}{1 + i\omega\tau} \right) \left(1 - \frac{i(kl)^2}{\gamma\omega\tau} (1 + i\gamma\omega\tau) \right) \right]^{-1}$$

$$\text{where } \gamma = 1 + \frac{a}{\pi c} \frac{\kappa_1}{\mu} \left(\frac{\lambda + 2\mu}{\lambda + \mu} \right) \text{ and } \tau = \frac{\phi_m l^2 \eta_l}{K_m \kappa_l};$$

λ and μ are the Lamé constants, ω and k are the angular frequency and wavenumber of the seismic wave, l is the interinclusion distance, a/c is the inclusion aspect ratio, κ_l and η_l are the bulk modulus and viscosity of the liquid, and ϕ_m and K_m are the porosity and permeability of the background matrix, respectively. Similarly, for the shear modulus, $\mu = \mu_0 + \phi\mu_1$, where

$$\frac{\mu_1}{\mu_0} = -\frac{2}{15} \left[\frac{8}{3} \left(\frac{\lambda + 2\mu}{\lambda + \mu} \right) \left(\frac{1 + i\omega\tau}{1 + i\gamma\omega\tau} \right) + 16 \left(\frac{\lambda + 2\mu}{3\lambda + 4\mu} \right) \left\{ 1 + \frac{4a}{\pi c} \frac{i\omega\eta_l}{\mu} \left(\frac{\lambda + 2\mu}{3\lambda + 4\mu} \right) \right\} \right]^{-1}$$

We use the definition of attenuation as the ratio of imaginary (*Im*) to real (*Re*) parts of these expres-

sions, and the corresponding *P*- and *S*-wave attenuation can then be defined as $Q_p^{-1} = \text{Im}(\kappa + 4\mu/3)/\text{Re}(\kappa + 4\mu/3)$ and $Q_s^{-1} = \text{Im}(\mu)/\text{Re}(\mu)$, respectively. Fixed parameters used in attenuation calculation (Fig. 4; Web fig. 3): $\lambda_0 = 941$ GPa, $\mu_0 = 636$ GPa, $\omega = 2\pi$, $kl = 10^{-6}/\phi$, $\phi_0 = 0.1$, $\kappa_f = 900$ GPa, and $K_m = 10^{-18}$ m².

41. R. A. Secco, *Mineral Physics and Crystallography: A Handbook of Physical Constants* (American Geophysical Union, Washington, DC, 1995), pp. 218–226.
 42. D. Gubbins, *Geophys. J.* **43**, 453 (1977).
 43. G. A. Glatzmaier and P. H. Roberts, *Int. J. Eng. Sci.* **36**, 1325 (1998).
 44. We thank J. Hudson and L. Stixrude for helpful discussions and comments on the manuscript. Supported by the European Commission, and additionally by the UK Natural Environment Research Council and the Institut de Physique du Globe de Paris (IPGP) (S.C.S. and J.P.M.). This paper is IPGP contribution no. 1658.

2 December 1999; accepted 14 February 2000

Insect Population Control Using a Dominant, Repressible, Lethal Genetic System

Dean D. Thomas,¹ Christl A. Donnelly,² Roger J. Wood,³ Luke S. Alphey^{1*}

A major modification to the sterile insect technique is described, in which transgenic insects homozygous for a dominant, repressible, female-specific lethal gene system are used. We demonstrate two methods that give the required genetic characteristics in an otherwise wild-type genetic background. The first system uses a sex-specific promoter or enhancer to drive the expression of a repressible transcription factor, which in turn controls the expression of a toxic gene product. The second system uses non-sex-specific expression of the repressible transcription factor to regulate a selectively lethal gene product. Both methods work efficiently in *Drosophila melanogaster*, and we expect these principles to be widely applicable to more economically important organisms.

The sterile insect technique (SIT) is a species-specific and environmentally nonpolluting method of insect control that relies on the mass rearing, sterilization, and release of large numbers of insects (1, 2). Released sterile males mate with wild females, reducing their reproductive potential and, ultimately, if enough males are released for a sufficient time, totally eradicating the pest population. Successful, area-wide SIT programs have been conducted against the screwworm fly *Cochliomyia hominivorax* (2), the Mediterranean fruit fly (Medfly) *Ceratitis capitata* (3), and the tsetse fly (*Glossina* spp.) (4).

Mass-rearing facilities initially produce equal numbers of the two sexes, but females are generally separated and discarded before release. Sterilized females are not thought to help control efforts and may indeed be detrimental to them (5). Mechanical sex-separation methods using pupal mass, time of eclosion, and so forth rarely yield a true single-sex population. Various female-killing and sex-sorting genetic systems have been developed, known generically as genetic sexing mechanisms (GSMs). So far, all GSMs in factory production have used radiation-induced translocations to the Y chromosome as dominant selectable markers, complementing an X-linked or autosomal recessive trait such as pupal color, temperature-sensitive lethality, blindness, or insecticide resistance (5–7). These chromosome aberration-based systems tend to be unstable and reduce the fitness of the insects, making them less effective agents for SIT (5).

A better approach would be to use a transgene system to induce repressible female-specific lethality. This could be used simply as a GSM. In addition, these transgenics could be used in a control program without requiring sterilization by irradiation. We call this variant of SIT “release of insects carrying a dominant lethal” (RIDL), because the insects are not, strictly speaking, sterile. RIDL requires that a strain of the target organism carries a conditional, dominant, sex-specific lethal, where the permissive condition can be created in the laboratory or factory but will never be encountered by the wild population. An ideal example would be a chemical additive to the diet.

To demonstrate the feasibility of RIDL, we attempted to construct the system in *Drosophila melanogaster*. We used *Drosophila* transcriptional control elements to drive expression of the tetracycline-repressible transactivator fusion protein (tTa) (8). In the absence of tetracycline, tTa will drive expression of any gene controlled by the tetracycline-responsive element (tRe). We first expressed tTa under the control of the Yp3 fat-body enhancer (9). This drives expression in female larvae and adults, but not in males (10, 11). Because yolk proteins or vitellogenins are expressed in a similar pattern in most insects, we expect these promoters to be useful for RIDL in insects of economic importance. To test for female-specific tTa expression, we used a tRe-lacZ reporter (12).

Flies homozygous for stable insertions of Yp3-tTa or tRe-lacZ were crossed to each other. The resulting progeny were raised either on normal media or on media supplemented with tetracycline. Adult abdomens were dissected and stained for lacZ activity. Females raised on normal media showed strong staining of the fat body, whereas females raised on tetracycline, and all males, were negative (13).

¹Department of Zoology, ²Wellcome Trust Centre for the Epidemiology of Infectious Disease, Department of Zoology, University of Oxford, South Parks Road, Oxford OX1 3PS, UK. ³School of Biological Sciences, University of Manchester, Manchester M13 9PT, UK.

*To whom correspondence should be addressed. E-mail: Luke.Alphey@zoo.ox.ac.uk